Journal of Magnetism and Magnetic Materials 475 (2019) 152–159

Contents lists available at ScienceDirect

Journal of Magnetism and Magnetic Materials

journal homepage: www.elsevier.com/locate/jmmm

Research articles

Investigation on the self-assembly of magnetic core-shell nanoparticles under soft-magnet element by using discrete element method

Zongqian Shi[a,*], Jiajia Sun[a], Shuang Chen[a], Shenli Jia[a]

[a] State Key Laboratory of Electrical Insulation and Power Equipment, Xi'an Jiaotong University, No. 28 Xianning West Road, Xi'an, Shaanxi Province 710049, China

ARTICLE INFO

Keywords:
Magnetic nanoparticles
Self-assembly
Soft-magnetic elements
Discrete element method

ABSTRACT

The self-assembly of magnetic core-shell nanoparticles in the presence of a magnetic template, which consists of an array of soft-magnetic elements embedded in non-magnetic substrate, is analyzed by using discrete element method. An external bias magnetic field is used to magnetize the soft-magnetic elements to saturate state. The high-gradient field produced by elements combined with biased uniform magnetic field provides a flexible way to control the behavior of particles. An equivalent source method is adopted to obtain the closed-form magnetic field analysis, which not only improves the calculation efficiency but also enables accurate prediction of the Kelvin force. In the presence of magnetic field, the behavior of the magnetic nanoparticles is dependent on the magnetic and hydrodynamic forces. Therefore, the assembled structures of magnetic nanoparticles are firstly investigated without considering the magnetic dipole interaction force, in which an unordered nanostructure is formed. As a contrast, the self-assembly of particles is also simulated by taking all forces into account. In this case, the magnetic nanoparticles assemble into an ordered 3D structure, which presents a hexagonal close packed structure. A comparison between the results of the mentioned two cases denotes that the magnetic dipole interaction force plays an important role in controlling the self-assembly of magnetic nanoparticles.

1. Introduction

Recently, the interests of bottom-up fabrication of nanostructures have attracted more attention for different fields, involving photon, micro-optics, magnetic and electric materials [1–3]. To date, various methods have been introduced to assemble nanoparticles into different patterns. Most of the methods are templates-assisted or directed assembly, and abundant experiments have been carried out to control the self-assembly of nanoparticles with nanoscale or microscale resolution [4–5]. The self-assembly of magnetic nanoparticles, in the control of external magnetic field, is regarded as the most promising method for implementing the adjustability of nanostructure. However, the intrinsic mechanism of self-assembly of magnetic nanoparticles still remain less known, and little work is carried out to investigate the reconfigurable assembly of the 3D nanostructure [6].

The self-assembly of magnetic nanoparticles in the presence of magnetic field is a complicated physical process, which is related to magnetic and hydrodynamic forces, including magnetic dipole-dipole interactions, van der Walls interaction, viscous force, Brownian motion, and the effects of surfactant force. Thus, different computational methods have been proposed to investigate the dynamic process of the self-assembly, including lattice-Boltzmann method [7], Monte Carlo, Langevin method [5], and molecular dynamic simulations, etc. [8].

Furlani introduced a template-assisted assembly method, in which soft-magnetic elements embedded into a nonmagnetic substrate are adopted to produce the external magnetic field as shown in Fig. 1 [4]. The external bias magnetic field $\boldsymbol{H}_{\text{bias}}$ was used to magnetize the soft-magnetic elements to saturate state. Besides, the soft-magnetic element could return to nonmagnetic state by removing the external magnetic field, which implements the function of switching on/off. That is to say, the assembly process is reversible and the nanoparticles can be redispersed once removing the external bias field.

In this study, the self-assembly process of magnetic core-shell nanoparticles in the presence of a magnetic template (as shown in Fig. 1) is analyzed by using discrete element method (DEM). The equivalent current source method, which is deduced from the magnetostatic field theory with the hypothesis that the magnetization of the magnet is constant, is adopted to analyze the spatial distribution of magnetic field [9]. This closed-form analysis of magnetic field enables accurate prediction of the Kelvin force, which can be derived by regarding the magnetic core of a nanoparticle as an equivalent magnetic dipole [10]. In order to investigate the influence of the hydrodynamic forces, two cases are considered to predict the assembly structure in the presence of same external magnetic field. In the first case, the self-assembly of

* Corresponding author.
E-mail address: zqshi@mail.xjtu.edu.cn (Z. Shi).

https://doi.org/10.1016/j.jmmm.2018.11.038
Received 17 May 2018; Received in revised form 29 October 2018; Accepted 5 November 2018
Available online 08 November 2018
0304-8853/

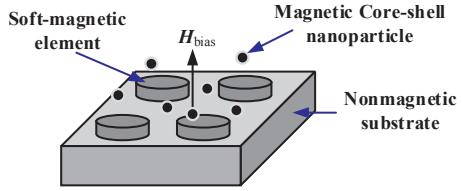

Fig. 1. The self-assembly system with soft-magnetic elements embedded in nonmagnetic substrate.

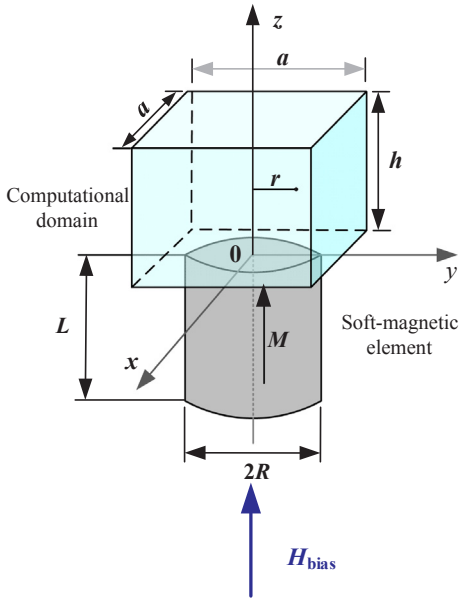

Fig. 2. The schematic diagram of a soft-magnetic element.

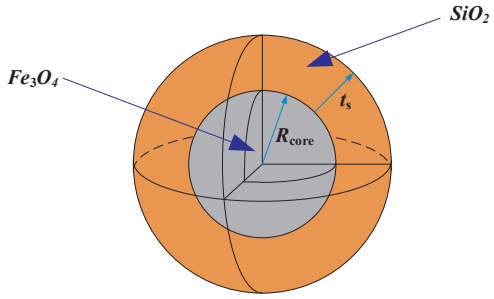

Fig. 3. The schematic diagram of a core-shell nanoparticle, and the materials of the core and the shell are Fe_3O_4 and SiO_2, respectively.

magnetic core-shell nanoparticles is demonstrated under the control of forces without the magnetic dipole interaction force. As a contrast, the assembly process of the nanoparticles is also predicted by considering all forces. The assembled nanostructures can be transferred to other substrate by using the method introduced by Henderson et al. [11]. As such, the proposed method in this work is potential in implementing bottom-up fabrication of functional 3D nanostructured materials.

2. Theoretical and computational model

In the presence of external magnetic field, magnetized magnetic nanoparticles could be attracted toward the region with high magnetic energy. Furthermore, the magnetic dipole interaction between magnetized particles could also induce the formation of ordered nanostructure. Then, the discrete element method is proposes to predict the self-assembly of magnetic nanoparticles under a cylindrical soft-magnetic element and bias magnetic field.

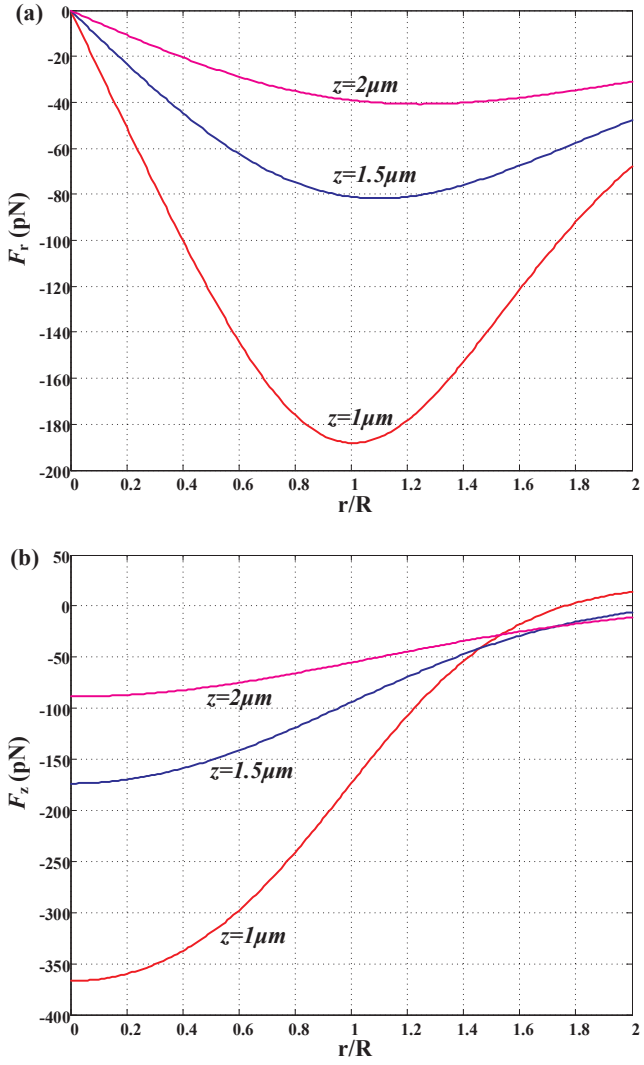

Fig. 4. The distribution of the radial (a) and axial (b) component of Kelvin force.

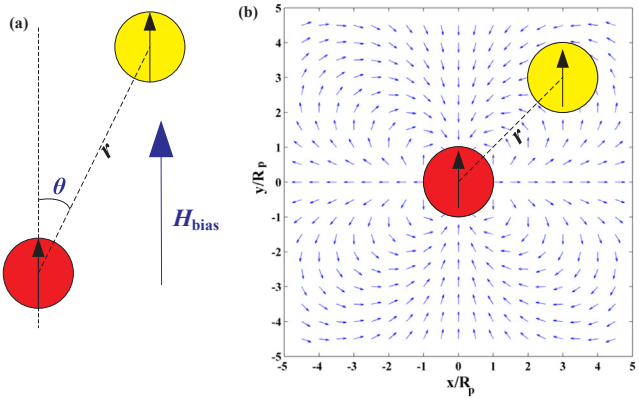

Fig. 5. The schematic of two interacting dipole (a), the normalized magnetic dipole interaction force field (b).

2.1. Discrete element method

By segmenting of the computation domain into a series of small cells, the trajectories of nanoparticles are calculated by loading the interaction forces $\boldsymbol{F}_{int}$ and the body force $\boldsymbol{F}_{body}$ into each cell. The Newtonian law is used to predict the self-assembly of magnetic

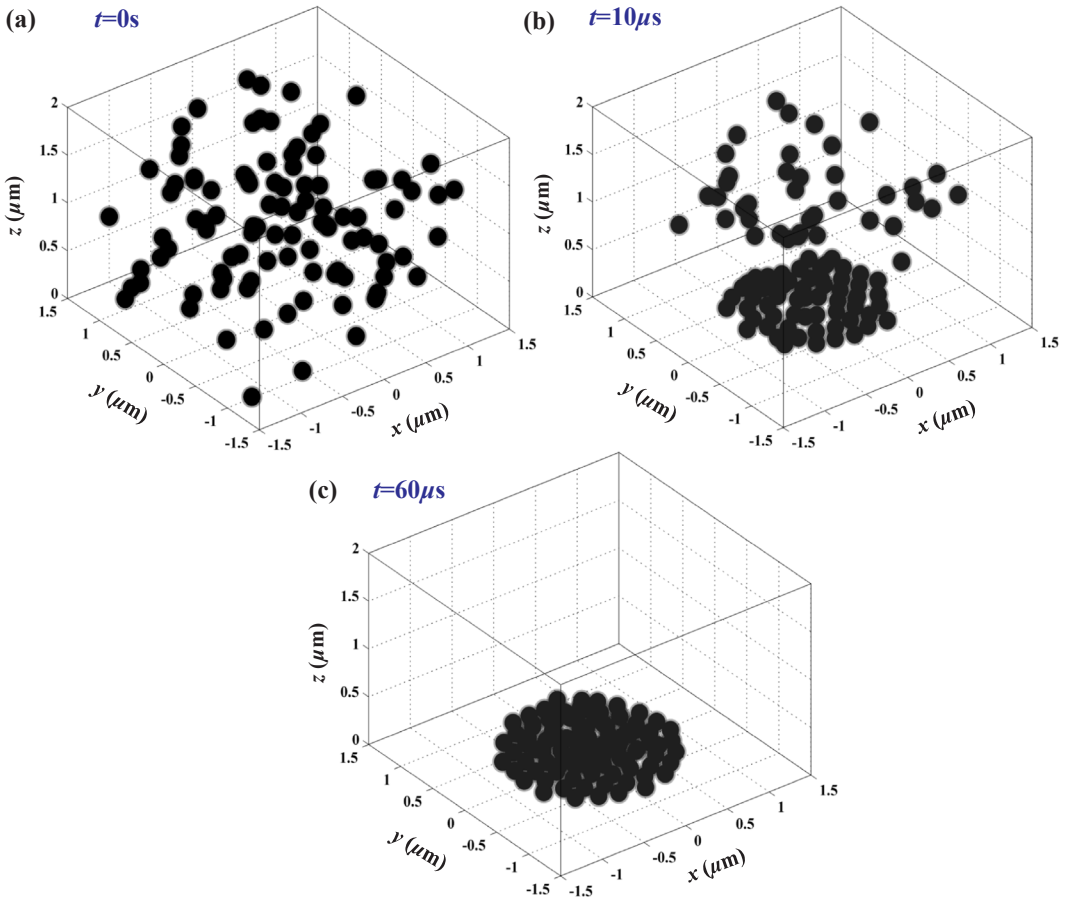

Fig. 6. The self-assembly of magnetic nanoparticles with c = 1.55% at different time: (a) t = 0 s, (b) t = 10 μs, (c) t = 60 μs without considering the magnetic dipole interaction force.

nanoparticles as shown in Eq. (1) [1,12],

$$m_i \frac{d^2 \boldsymbol{x}_i}{dt^2} = \boldsymbol{F}_{body} + \boldsymbol{F}_{\text{int}} \tag{1}$$

where

$$\begin{aligned} \boldsymbol{F}_{body} &= \boldsymbol{F}_{m,i} + \boldsymbol{F}_{vis,i} + \boldsymbol{F}_{B,i} \\ \boldsymbol{F}_{\text{int}} &= \sum_{\substack{j=1 \\ j\neq i}}^{N} (\boldsymbol{F}_{dd,ij} + \boldsymbol{F}_{vdw,ij} + \boldsymbol{F}_{surf,ij} + \boldsymbol{F}_{hyd,ij}) \end{aligned} \tag{2}$$

The m_i and x_i are the mass and position of i'th particle. $\boldsymbol{F}_{m,i}$, $\boldsymbol{F}_{vis,i}$ and $\boldsymbol{F}_{B,i}$ are the Kelvin force, viscous force and Brownian Force, respectively. The $\boldsymbol{F}_{dd,ij}$, $\boldsymbol{F}_{vdw,ij}$, $\boldsymbol{F}_{surf,ij}$, and $\boldsymbol{F}_{hyd,ij}$ are the magnetic dipole–dipole interaction force, van der Waals force, the surfactant force and hydrodynamic interactions force between ith particle and jth particle, respectively.

At first, the acceleration of particles is obtained by solving Eq. (1). Then, the velocity and location of particles are achieved via integrating the acceleration equation by using central difference method. It is worth noting that the interaction force between the particles is only included in the conditions when the distance between two particles is smaller than a threshold (d_c).

2.2. Magnetic field

The magnetic field of a soft-magnetic permalloy element (78% Ni 22% Fe, $M_s = 8.6 \times 10^5$ A/m) is analyzed by using equivalent current source method, which is introduced by Furlani [13]. As shown in Fig. 2, the x-y plane of the coordinate is coincident with the top surface of the magnet, with R = 1 μm and L = 3 μm. The x, y, and z are used to indicate the coordinate of a particle. The r and z are adopted to describe the distribution of the magnetic field. The a and h are the length and height of computational domain with a = 3 μm and h = 2 μm.

The magnet density flux of a soft-magnetic element, which is magnetized by the bias magnetic field $\boldsymbol{H}_{\text{bias}}$, can be given as the Eq. (3).

$$\boldsymbol{B} = B_r \boldsymbol{e}_r + B_z \boldsymbol{e}_z \tag{3}$$

where B_r and B_z are the radical and axial component of B. A cylindrical neodymium–iron–boron (NdFeB) magnet with radius 6 mm and height 8 mm is used to produce the bias field ($H_{\text{bias}} = 3.9 \times 10^5$ A/m), which is ideal to magnetize the soft-magnetic element to saturate state [6].

$$B_r = \frac{\mu_0 M_s}{2\pi} \times \int_{-L}^{0} \frac{z - z'}{r[(R+r)^2 + (z-z')^2]^{1/2}} \cdot \left[\frac{R^2 + r^2 + (z-z')^2}{(R-r)^2 + (z-z')^2} \cdot E(k) - K(k) \right] dz' \tag{4}$$

$$B_z = \mu_0 H_{bias} + \frac{\mu_0 M_s}{2\pi} \times \int_{-L}^{0} \frac{1}{[(R+r)^2 + (z-z')^2]^{1/2}} \cdot \left[\frac{R^2 - r^2 - (z-z')^2}{(R-r)^2 + (z-z')^2} \cdot E(k) + K(k) \right] dz' \tag{5}$$

where r' and z' are the coordinate of a point at the lateral surface of magnet, and K(k), E(k) are the complete elliptic integrals of the first and second kind, respectively [14].

$$K(k) = \int_0^{\frac{\pi}{2}} \frac{1}{\sqrt{1 - k^2 \sin^2 \Phi}} d\Phi, \quad E(k) = \int_0^{\frac{\pi}{2}} \sqrt{1 - k^2 \sin^2 \Phi}\, d\Phi \tag{6}$$

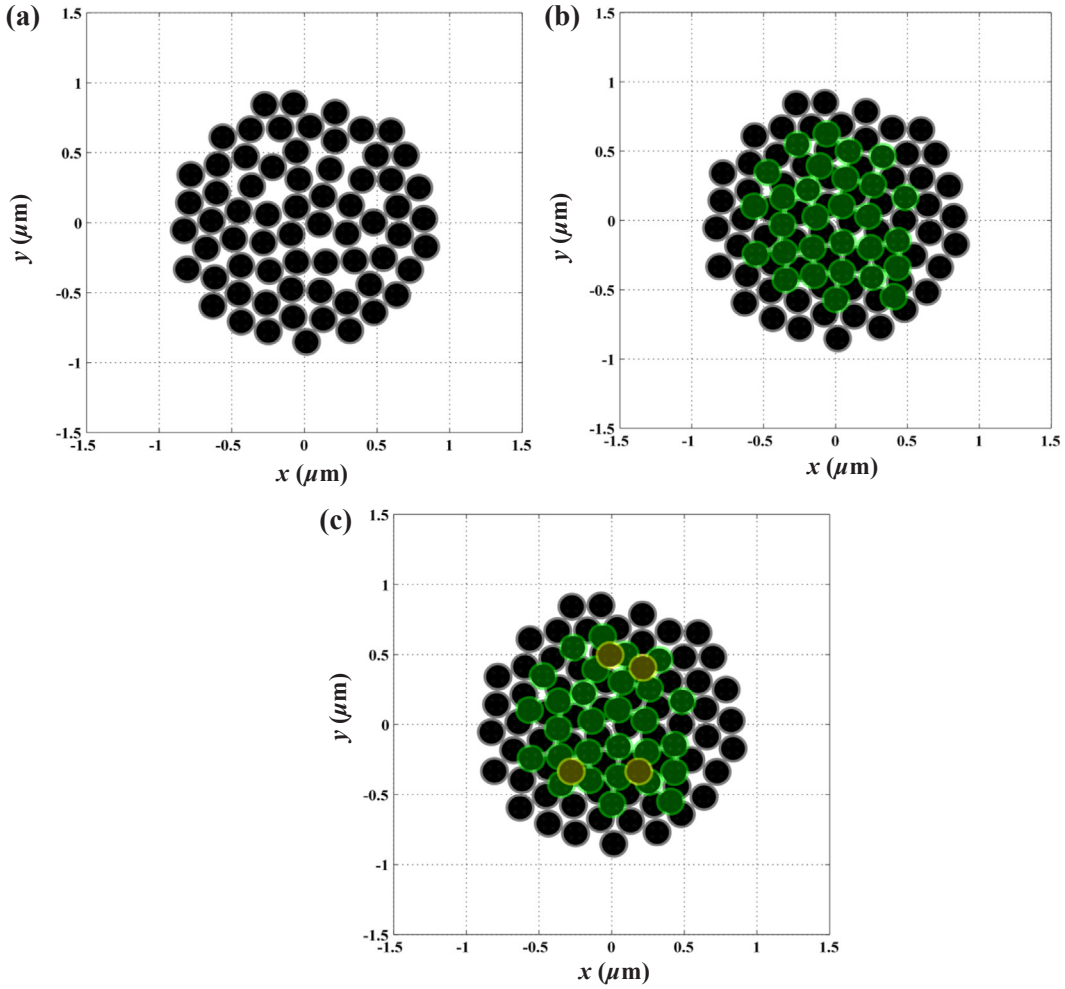

Fig. 7. The assembled nanostructure at the bottom of the computational domain, (a) the first layer (black), (b) the second layer (green), (c) the third layer (yellow) without considering the magnetic dipole interaction force. (For interpretation of the references to color in this figure legend, the reader is referred to the web version of this article.)

2.3. Kelvin force

The Kelvin force on magnetic core-shell nanoparticles can be obtained by regarding the magnetic core of a particle as equivalent magnetic dipole with an effective moment $\boldsymbol{m}_{\mathrm{p,eff}}$, as shown in Eq. (7) [15].

$$\boldsymbol{F}_m = \mu_f (\boldsymbol{m}_{p,eff} \cdot \nabla)\boldsymbol{H} \tag{7}$$

where μ_f is the permeability of the fluid and $\boldsymbol{H}$ is the magnetic field at the center of the particles. Taking the self-demagnetization and particle saturation into consideration, the effective magnetic moment can be written as [16]

$$\boldsymbol{m}_{p,eff} = V_p f(\boldsymbol{H})\boldsymbol{H} \tag{8}$$

where

$$f(\boldsymbol{H}) = \begin{cases} \frac{3(\chi_p - \chi_f)}{(\chi_p + 2\chi_f) + 3} & H < \left(\frac{(\chi_p + 2\chi_f) + 3}{3(\chi_p - \chi_f)}\right) M_{sp} \\ M_{sp}/H & H > \left(\frac{(\chi_p + 2\chi_f) + 3}{3(\chi_p - \chi_f)}\right) M_{sp} \end{cases} \tag{9}$$

In this expression, the χ_{p} and χ_f are the susceptibility of magnetic core and fluid, respectively. The V_{p} is the volume of nanoparticle, and M_{sp} is the saturation magnetization of particle.

2.4. Magnetic dipole interaction force

Under the external magnetic field, a magnetized magnetic nanoparticle with dipole moment $\boldsymbol{m}_{\mathrm{i,eff}}$, could impose an interaction force on the particles that are close to it. The dipole interaction force is obtained by the gradient of potential energy of dipole-dipole interaction $U_{\mathrm{dd,ij}}$ as [4]

$$\boldsymbol{F}_{dd,ij} = -\nabla U_{dd,ij}$$
$$U_{dd,ij} = -\frac{\mu_f}{4\pi}\left(3\frac{(\boldsymbol{m}_{i,eff}\cdot\boldsymbol{r}_{ij})(\boldsymbol{m}_{j,eff}\cdot\boldsymbol{r}_{ij})}{r_{ij}^5} - \frac{\boldsymbol{m}_{i,eff}\cdot\boldsymbol{m}_{j,eff}}{r_{ij}^3}\right) \tag{10}$$

where $\boldsymbol{m}_{\mathrm{i,eff}}$ and $\boldsymbol{m}_{\mathrm{j,eff}}$ are the dipole moment of particle i and j, respectively. The $\boldsymbol{r}_{\mathrm{ij}}$ is the displacement vector between them.

2.5. Van der Waals interaction force

The Van Der Waals interaction force is given as [4]

$$F_{vdw,ij} = \frac{A}{6}\frac{d_i^6}{(h_{ij}^2 + 2d_i h_{ij})^2 (h_{ij} + d_i)^3} \tag{11}$$

where A is the *H*amaker constant, $A = 4 \times 10^{-19}$ J and h_{ij} is the surface-to-surface distance between the ith and jth particle. The d_{i} is the diameter of ith particle.

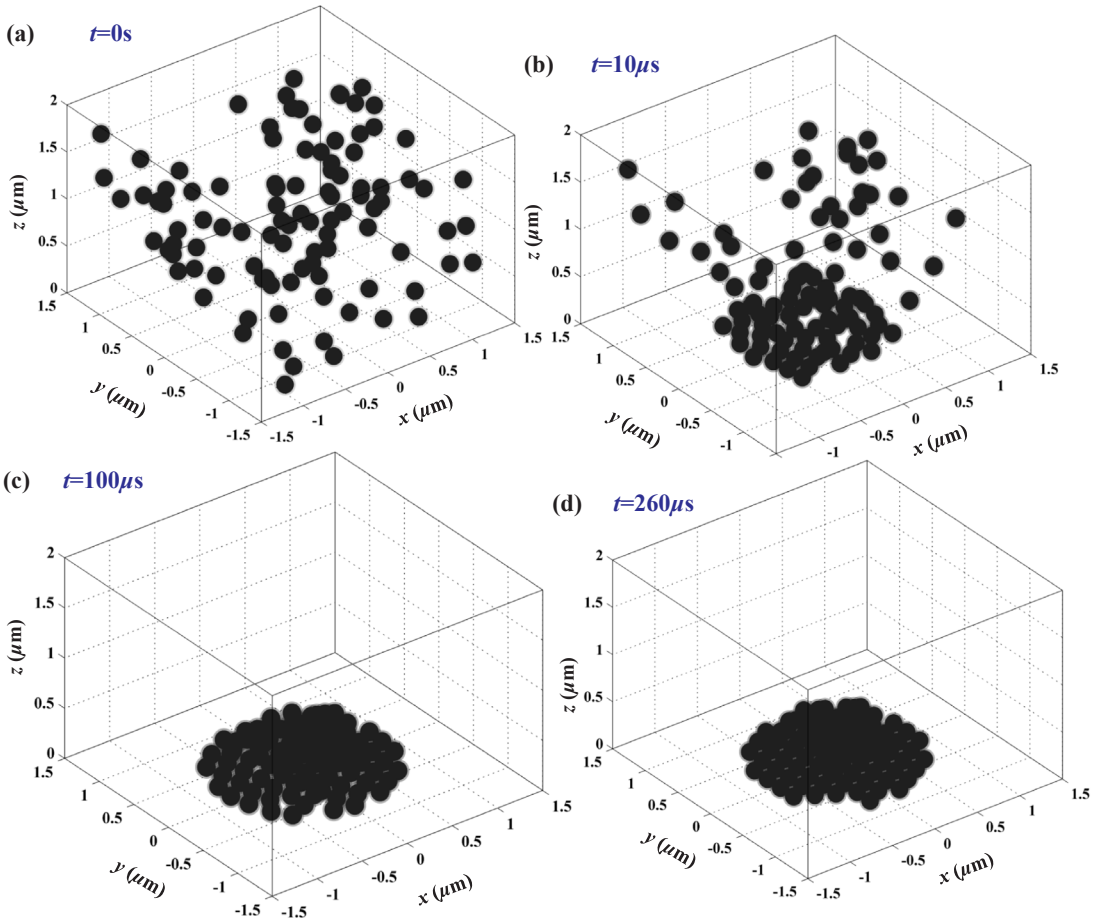

Fig. 8. The self-assembly of magnetic nanoparticles with $c = 1.55\%$ at different time: (a) $t = 0$ s, (b) $t = 10$ μs, (c) $t = 100$ μs, (d) $t = 260$ μs with considering all forces.

2.6. Surfactant force

Due to the interaction of surfactant-surfactant, the repulsive surfactant force is calculated by using [4]

$$F_{surf,ij} = -\nabla U_s$$
$$U_s = \frac{\pi R_p^2 N_s k_B T}{2}\left\{2 - \frac{r_{ij} - 2R_p}{\delta} - \frac{r_{ij}}{\delta}\ln\left(\frac{2R_p + 2\delta}{r_{ij}}\right)\right\} \quad (12)$$

where U_s, R_p, N_s, δ are the potential energy of surfactant-surfactant interaction, radius of particles, the surface density of surfactant molecules, and the thickness of surfactant layer. $N_s = 1 \times 10^{19}$ molecules/m^2, and $\delta = 1$ nm. The k_B and T are the Boltzmann's constant and temperature, $k_B = 1.38 \times 10^{-23}$ J/K, $T = 298$ K.

2.7. Viscous drag force

Due to viscous of carrier fluid, the viscous drag force is given by Stokes' formula [5],

$$\boldsymbol{F}_{vis,i} = 6\pi\eta R_{hyd,p}\frac{d\boldsymbol{x}_i}{dt} \quad (13)$$

where η is the viscous of fluid, and $R_{hyd,p}$ is the hydrodynamic radius of particle, which is regarded to be the same as the particle radius.

2.8. Hydrodynamics' interaction force

The hydrodynamics' interaction force is written as shown in Eq. (14) based on the lubrication theory [5].

$$\boldsymbol{F}_{hyd,ij} = \frac{6\pi\mu_f \boldsymbol{V}_{r,i,j}}{h_{ij}}\cdot\frac{d_i^2}{16} \quad (14)$$

where $\boldsymbol{V}_{r,i,j}$ is the relative velocity between the particles.

2.9. Brownian force

The Brownian force is described by using Gaussian white process. The force in one dimension is [1]

$$F_B = \xi\sqrt{\frac{2Dk_BT}{\Delta t}} \quad (15)$$

where $D = 6\pi\eta R_{hyd,p}$ is the Strokes' drag coefficient, the Δt is the time step, the ξ is a random number with Gaussian distribution and its range is $(-1, 1)$.

3. Results and discussions

The core-shell nanoparticles with $R_{core} = 80$ nm and $t_s = 20$ nm are adopted as shown in Fig. 3. The material of the core is assumed to be Fe_3O_4 with $M_{sp} = 4.78 \times 10^5$ A/m, $\rho_{core} = 5000$ kg/m^3, and $\chi_p = 1.4$. Considering the material of carrier fluid (water, $\chi_f = 0$), the Eq. (9) can be simplified as follows,

$$f(H) = \begin{cases} \frac{3\chi_p}{\chi_p + 3} & H < \left(\frac{\chi_p + 3}{3\chi_p}\right)M_{sp} \\ M_{sp}/H & H \geqslant \left(\frac{\chi_p + 3}{3\chi_p}\right)M_{sp} \end{cases} \quad (16)$$

The material of shell of the particles is assumed to be SiO_2, with

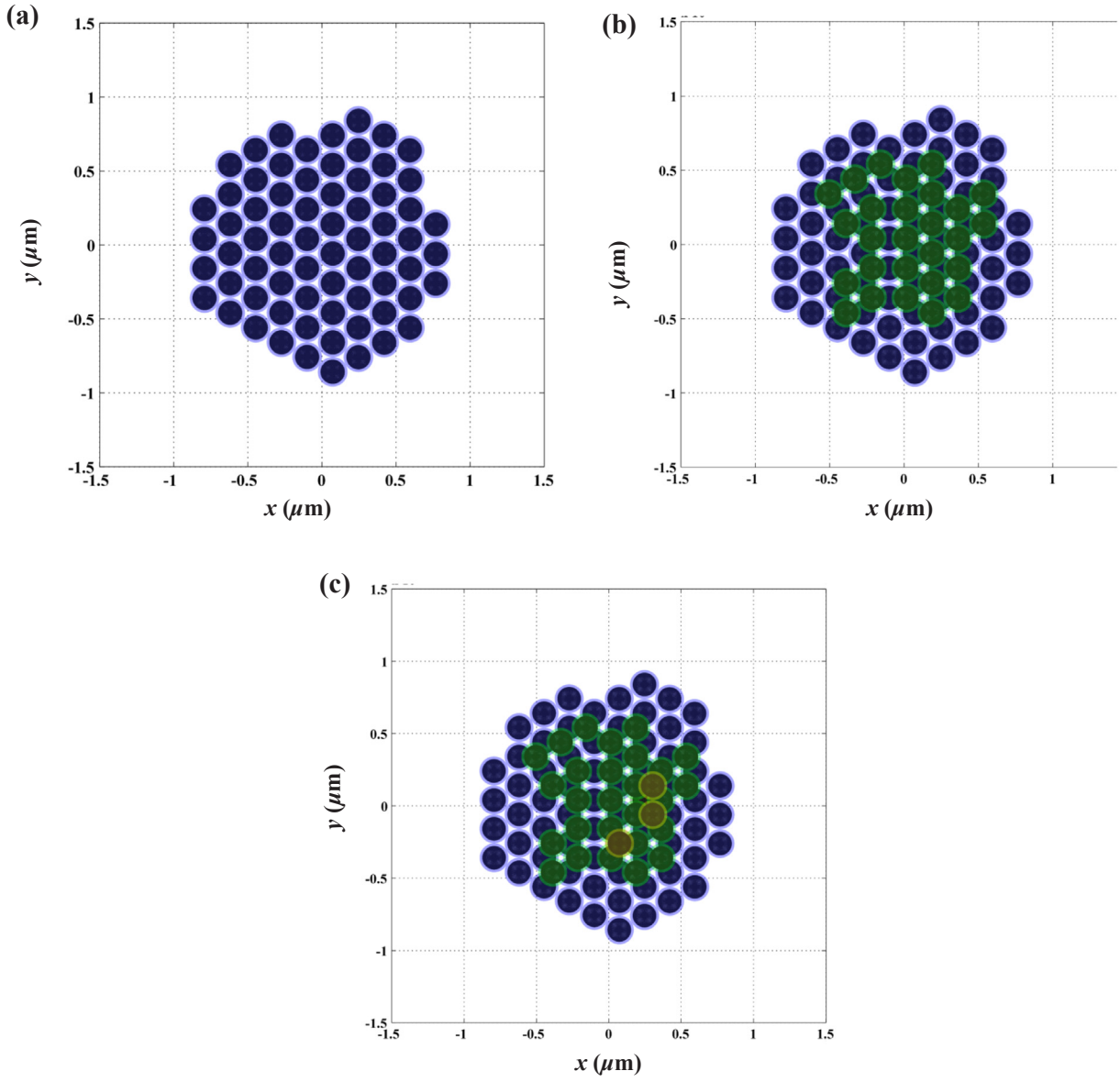

Fig. 9. The assembled nanostructure at the bottom of the computational domain, (a) the first layer (blue), (b) the second layer (green), (c) the third layer (yellow) considering all forces. (For interpretation of the references to color in this figure legend, the reader is referred to the web version of this article.)

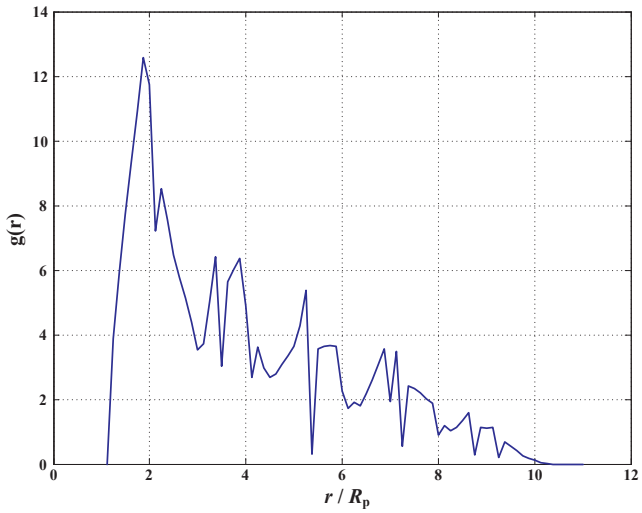

Fig. 10. The distribution of radial distribution function g(r) as a function of r.

$\rho_{shell} = 2648\ kg/m^3$. The carrier fluid is assumed to be water with $\eta = 0.001\ N{\cdot}s/m^2$ and $\rho_f = 1000\ kg/m^3$.

A magnetic template consisting of an array of soft-magnetic elements is adopted to produce the external magnetic field as shown in Fig. 1. The center-to-center distance between the elements is 40 μm so that there is no overlap in their individual magnetic field. The distribution of the Kelvin force in the presence of a soft-magnetic element is investigated at first as shown in Fig. 4. An external bias magnetic field $\boldsymbol{H}_{bias}$ is adopted to magnetize the soft-magnetic element to saturate state.

As shown in Fig. 4(a), for a given z, the amplitude of F_{mr} increases with the increase of r, and obtains maximum near the margin of the magnet, from where it decreases with the increase of r. Specially, the radial force is negative and plays an important role in focusing the particles towards the center of computational region.

The amplitude of the axial force F_{mz} obtains maximum at the center of the element and decreases with the increase of r at a given z as shown in Fig. 4(b). Moreover, it should be noted that the F_{mr} and F_{mz} is negative and decreases with the increase of z. This denotes that in the influence of Kelvin force, the particles are directed downward towards

the center of the top surface of the magnet. Furthermore, with regard to the particles that far from the element, the Kelvin force is too weak to control the behavior of particles, so that the magnetic interaction between particles plays a significant role in influencing the self-assembly of particles. Therefore, it is essential to investigate the influence of the interaction forces on the behavior of the particles.

The evolution of the magnetic dipole interaction force between two particles is investigated in the presence of a uniform magnetic field as shown in Fig. 5(a) [5]. To simply the analysis, one particle (red) is assumed to be fixed at the origin of the coordinate. The normalized magnetic dipole force on another second particle (yellow) as a function of its location is analyzed as shown in Fig. 5(b).

From the Fig. 5(b), we can derive that the magnetic dipole interaction force varies from attractive force (moving towards the first particle) to repulsive force (far away from the first particle) with the change of the angle θ. As the center-to-center distance $\boldsymbol{r}$ is parallel to the x axis, the $\boldsymbol{F}_{\mathrm{dd,ij}}$ is a repulsive force, whereas it is an attractive force as $\boldsymbol{r}$ is perpendicular to the x axis. This short range interaction force $F_{\mathrm{dd,ij}}$ strengths the reciprocity between particles and contributes to the formation of the ordered nanostructure.

Then, the self-assembly of magnetic nanoparticles in the presence of a soft-magnetic element is simulated by using discrete element method with a constant time step $\Delta t = 1$ns. The threshold distance d_c is chosen as $10R_p$. The initial volume fraction of particles is $c = 1.55\%$ and the particles are randomly distributed. Without considering the magnetic dipole interaction force, the dynamic assembly process of the magnetic nanoparticles is simulated as shown in Fig. 6.

As time goes on, most of the magnetic nanoparticles are gradually attracted towards the magnetic source and accumulate at the center of the bottom of the computational domain. At $t = 60$ μs, all of the particles are captured and form an unordered nanostructure. The final stacked profiles with color-coded particles packing in different layers are shown in Fig. 7.

As shown in Fig. 7(a), there are some obvious interspaces in the first layer of the nanostructure, which are not filled by the particles from the second layer. This implies that the Kelvin force makes little contribution to the formation of the ordered nanostructure, which is implemented by the interaction force. In the theory of Faraudo et al., the significance of magnetic dipole interaction in the process of self-assembly of particles can be predicted by using aggregation parameter N^* [17],

$$N^* = \sqrt{c_0 e^{\Gamma-1}} \tag{17}$$

where c_0 is initial volume fraction of particle and Γ is magnetic coupling parameter [18]

$$\Gamma = \frac{\mu_0 M_{p,v}^2 V_p}{12 k_B T} \tag{18}$$

where $M_{\mathrm{p,v}}$ and V_{p} are volumetric magnetization and volume of magnetic core. Considering the particle with $R_{\mathrm{core}} = 80$ nm and $R_{\mathrm{p}} = 100$ nm, the magnetic coupling parameter Γ is 3.7×10^4, which results in $N^* \gg 1$. This implies that the magnetic dipole interaction should be taken into consideration in predicting the self-assembly of magnetic nanoparticles [19].

Next, by taking the magnetic dipole interaction force into consideration, the dynamic assembly process of the magnetic nanoparticles is investigated as shown in Fig. 8.

In the presence of a soft-magnetic element, most of the particles are directed towards the bottom of the computational domain with time going on. The final assembly is completed at $t = 260$ μs and presents an ordered profile with partially populated three layers. Then, the color-labelled packing of the assembled particles at different layers is shown in Fig. 9, from which a hexagonal close packed structure can be observed. A comparison between the assembled structure of Figs. 7 and 9 implies that the magnetic dipole interaction force plays an important role in controlling the self-assembly of the particles.

Besides, in order to verify the influence of magnetic dipole interaction on the formation of hexagonal close packed structure, a radial distribution function g(r) is proposed to investigate the ordering of the self-assembled nanostructure.

$$g(r) = \frac{\Delta N}{\rho_{all} 4\pi r^2 \Delta r} \tag{19}$$

where ΔN is the number of particles in a spherical shell $4\pi r^2 \Delta r$, and ρ_{all} is the global density of particle number. In order to simply analysis, we only analyze the variation of g(r) for the particle captured at the bottom center. Furthermore, it should be noted that only the particles that are captured at the first layer are considered. As shown in Fig. 10, the profile of g(r) presents more peaks and obtains maximum at $r \approx 2R_{\mathrm{p}}$, implying a significant effect of magnetic dipole interaction on the formation of ordered structure.

Finally, it is worth noting that the self-assembled nanostructure could be transfer from soft-magnetic element to other substrate by using a heated polymeric coating and an acetone vapor as proposed by Furlani et al. [1].

4. Conclusion

The self-assembly of magnetic nanoparticle, suspending in water, in the presence of a magnetic template is simulated by using discrete element method. The magnetic template consisting of an array of soft-magnetic elements, which are embedded into non-magnetic substrate and can be magnetized to saturate state by using external bias magnetic field, is adopted to produce the magnetic field. The dynamic processes of the self-assembly of the magnetic nanoparticles under the external magnetic field are investigated in two cases.

In the first case, the magnetic dipole interaction force is not considered. An unordered assembled nanostructure of the nanoparticles is formed. As a contrast, taking all the force into account, the magnetic nanoparticles assemble into ordered 3D structure, which presents a hexagonal close packed structure. A comparison between the two cases denotes that the magnetic dipole interaction forces plays a significant role in affecting the self-assembly of magnetic nanoparticles.

Acknowledgements

The work was supported by the National Natural Science Foundation of China under project 51777148.

References

[1] K. Liu, X. Xue, V. Sukhotskiy, E.P. Furlani, Optical fano resonance in self-assembled magnetic-plasmonic nanostructures, J. Phys. Chem. C (2016).
[2] P. Alonso-Gonzalez, M. Schnell, P. Sarriugarte, H. Sobhani, C. Wu, N. Arju, A. Khanikaev, F. Golmar, P. Albella, L. Arzubiaga, F. Casanova, L.E. Hueso, P. Nordlander, G. Shvets, R. Hillenbrand, Real-space mapping of Fano interference in plasmonic metamolecules, Nano Lett. 11 (2011) 3922–3926.
[3] J.A. Fan, C. Wu, K. Bao, J. Bao, R. Bardhan, N.J. Halas, V.N. Manoharan, P. Nordlander, G. Shvets, F. Capasso, Self-assembled plasmonic nanoparticle clusters, Science 328 (2010) 1135.
[4] X. Xue, J. Wang, E.P. Furlani, Self-assembly of crystalline structures of magnetic core-shell nanoparticles for fabrication of nanostructured materials, ACS Appl. Mater. Interfaces 7 (2015) 22515–22524.
[5] X. Xue, E.P. Furlani, Analysis of the dynamics of magnetic core-shell nanoparticles and self-assembly of crystalline superstructures in gradient fields, J. Phys. Chem. C 119 (2015) 5714–5726.
[6] X. Xue, E.P. Furlani, Template-assisted nano-patterning of magnetic core-shell particles in gradient fields, Phys. Chem. Chem. Phys. 16 (2014) 13306–13317.
[7] Y. Xuan, M. Ye, Q. Li, Mesoscale simulation of ferrofluid structure, Int. J. Heat Mass Transfer 48 (2005) 2443–2451.
[8] Z. Wang, C. Holm, H.W. Muller, Molecular dynamics study on the equilibrium magnetization properties and structure of ferrofluids, Phys. Rev. E 66 (2002) 021405.
[9] E.P. Furlani, Permanent Magnet and Electromechanical Devices: Materials, Analysis, and Applications, Academic Press, 2001.
[10] Q. Cao, X. Han, L. Li, Numerical analysis of magnetic nanoparticle transport in microfluidic systems under the influence of permanent magnets, J. Phys. D: Appl. Phys. 45 (2012) 465001.

[11] J. Henderson, S. Shi, S. Cakmaktepe, T.M. Crawford, Pattern transfer nanomanufacturing using magnetic recording for programmed nanoparticle assembly, Nanotechnology 23 (2012) 185304.
[12] E.W.C. Lim, Gelation of Magnetic Nanoparticles, InTech, 2012.
[13] E.P. Furlani, K.C. Ng, Nanoscale magnetic biotransport with application to magnetofection, Phys. Rev. E 77 (2008).
[14] Z. Shi, J. Sun, S. Jia, P. Zhang, Simulation of magnetophoresis of magnetic nanoparticles in liquids, J. Phys. D: Appl. Phys. 49 (2016) 335005.
[15] E.P. Furlani, X. Xue, Field, force and transport analysis for magnetic particle-based gene delivery, Microfluid Nanofluid 13 (2012) 589–602.
[16] J. Sun, Z. Shi, S. Jia, P. Zhang, The force analysis for superparamagnetic nanoparticles-based gene delivery in an oscillating magnetic field, J. Magn. Magn. Mater. (2016).
[17] J.S. Andreu, J. Camacho, J. Faraudo, M. Benelmekki, C. Rebollo, L.M. Martínez, Simple analytical model for the magnetophoretic separation of superparamagnetic dispersions in a uniform magnetic gradient, Phys. Rev. E 84 (2011).
[18] J. Faraudo, J.S. Andreu, C. Calero, J. Camacho, Predicting the self-assembly of superparamagnetic colloids under magnetic fields, Adv. Funct. Mater. 26 (2016) 3837–3858.
[19] J. Faraudo, J.S. Andreu, J. Camacho, Understanding diluted dispersions of superparamagnetic particles under strong magnetic fields: a review of concepts, theory and simulations, Soft Matter 9 (2013) 6654.